

Particles in Fluids

Hans J. Herrmann^a José S. Andrade Jr.^b Ascânio D. Araújo^b

^a*IfB, ETH Zürich, Hönggerberg, 8093 Zürich, Switzerland.*

^b*Departamento de Física, Universidade Federal do Ceará,
60451-970 Fortaleza, Ceará, Brazil.*

Abstract

For finite Reynolds numbers the interaction of moving fluids with particles is still only understood phenomenologically. We will present three different numerical studies all using the solver “Fluent” which elucidate this issue from different points of view. On one hand we will consider the case of fixed particles, i.e. a porous medium and present the distribution of channel openings and fluxes. These distributions show a scaling law in the density of particles and for the fluxes follow an unexpected stretched exponential behaviour. The next issue will be filtering, i.e. the release of massive tracer particles within this fluid. Interestingly a critical Stokes number below which no particles are captured and which is characterized by a critical exponent of $1/2$.

1. Introduction

Particles in fluids (liquids or gases) appear in many applications in chemical engineering, fluid mechanics, geology and biology (1; 2; 3). Also fluid flow through a porous medium is of importance in many practical situations ranging from oil recovery to chemical reactors and has been studied experimentally and theoretically for a long time (4; 5; 6). Due to disorder, porous media display many interesting properties that are however difficult to handle even numerically. One important feature is the presence of heterogeneities in the flux intensities due the varying channel widths. They are crucial to understand stagnation, filtering, dispersion and tracer diffusion.

In the porous space the fluid mechanics is based on the assumption that a Newtonian and incompressible fluid flows under steady-state conditions. We consider the Navier-Stokes and continuity equations for the local velocity \vec{u} and pressure fields p , being ρ is the density of the fluid. No-slip boundary conditions are applied along the entire solid-fluid interface, whereas a uniform velocity profile, $u_x(0, y) =$

V and $u_y(0, y) = 0$, is imposed at the inlet of the channel. For simplicity, we restrict our study to the case where the Reynolds number, defined here as $Re \equiv \rho V L_y / \mu$, is sufficiently low ($Re < 1$) to ensure a laminar viscous regime for fluid flow. We use FLUENT (7), a computational fluid dynamic solver, to obtain the numerical solution on a triangulated grid of up to hundred thousand points adapted to the geometry of the porous medium.

The investigation of single-phase fluid flow at low Reynolds number in disordered porous media is typically performed using Darcy’s law (4; 6), which assumes that a *macroscopic* index, the permeability K , relates the average fluid velocity V through the pores with the pressure drop ΔP measured across the system,

$$V = -\frac{K}{\mu} \frac{\Delta P}{L}, \quad (1)$$

where L is the length of the sample in the flow direction and μ is the viscosity of the fluid. In previous studies (9; 10; 11; 12; 13; 14; 15), computational simulations based on detailed models of pore geometry and fluid flow have been used to predict permeability coefficients.

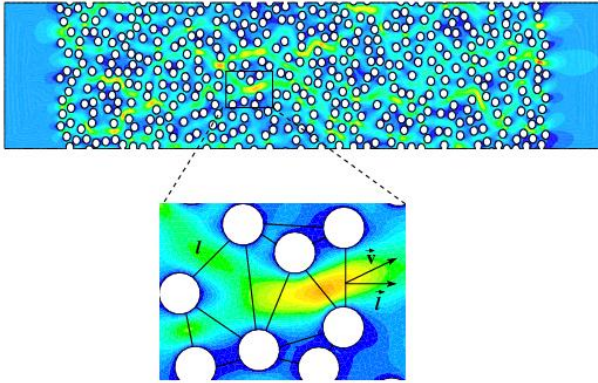


Fig. 1. Velocity magnitude for a typical realization of a pore space with porosity $\epsilon = 0.7$ subjected to a low Reynolds number and periodic boundary conditions applied in the y -direction. The fluid is pushed from left to right. The colors ranging from blue (dark) to red (light) correspond to low and high velocity magnitudes, respectively. The close-up shows a typical pore opening of length l across which the fluid flows with a line average velocity \bar{v} . The local flux at the pore opening is given by $q = vl \cos \theta$, where θ is the angle between \bar{v} and the vector normal to the line connecting the two disks.

Here we present numerical calculations for a fluid flowing through a two-dimensional channel of width L_y and length L_x filled with randomly positioned circular obstacles (16). For instance, this type of model has been frequently used to study flow through fibrous filters (24). Here the fluid flows in the x -direction at low but non-zero Reynolds number and in the y -direction we impose periodic boundary conditions. We consider a particular type of random sequential adsorption (RSA) model (17) in two dimensions to describe the geometry of the porous medium. As shown in Fig. 1, disks of diameter D are placed randomly by first choosing from a homogeneous distribution between $D/2$ and $L_x - D/2$ ($L_y - D/2$) the random x -(y -)coordinates of their center. If the disk allocated at this position is separated by a distance smaller than $D/10$ or overlaps with an already existing disk, this attempt of placing a disk is rejected and a new attempt is made. Each successful placing constitutes a decrease in the porosity (void fraction) ϵ by $\pi D^2/4L_xL_y$. One can associate this filling procedure to a temporal evolution and identify a successful placing of a disk as one time step. By stopping this procedure when a certain value of ϵ is achieved, we can produce in this way systems of well controlled porosity. We study in particular configurations with $\epsilon = 0.6, 0.7, 0.8$ and 0.9 .

2. Results on Filtration

Filtration is typically used to get clean air or water and also plays a crucial role in the chemical industry. For this reason it has been studied extensively in the past (18). In particular, we will focus here on deep bed filtration where the particles in suspension are much smaller than the pores of the filter which they penetrate until being captured at various depths. For non-Brownian particles, at least four capture mechanisms can be distinguished, namely, the geometrical, the chemical, the gravitational and the hydrodynamical one (18).

Very carefully controlled laboratory experiments were conducted in the past by Ghidaglia *et al.* (19) evidencing a sharp transition in particle capture as function of the dimensionless ratio of particle to pore diameter characterized by the divergence of the penetration depth. Subsequently, Lee and Koplik (20) found a transition from an open to a clogged state of the porous medium that is function of the mean particle size. Much less effort, however, has been dedicated to quantify the effect of inertial impact on the efficiency of a deep bed filter.

Here we will concentrate on the inertial effects in capture which constitute an important mechanism in most practical cases and, despite much effort, are quantitatively not yet understood, as reviewed in Ref. (21). The effect of inertia on the suspended particles is usually quantified by the dimensionless *Stokes number*, $St \equiv Vd_p^2\rho_p/18\ell\mu$, where d_p and ρ_p are the diameter and density of the particle, respectively, ℓ is a characteristic length of the pores, μ is the viscosity and V is the velocity of the fluid. Inertial capture by fixed bodies has already been described since 1940 by Taylor and proven to happen for inviscid fluids above a critical Stokes number (22). It is our aim to present a detailed hydrodynamic calculation of the inertial capture of particles in a porous medium. We will disclose novel scaling relations.

Let us first consider the case of an infinite ordered porous medium composed of a periodic arrangement of fixed circular obstacles (e.g., cylinders) (23). This system can then be completely represented in terms of a single square cell of unitary size and porosity given by $\epsilon \equiv (1 - \pi D^2/4)$, where D is the diameter of the obstacle, as shown in Fig. 1. Assuming Stokesian flow through the void space an analytical solution has been provided by Marshall *et al.* (24). Here we use this solution to obtain the velocity flow field \mathbf{u} and study the transport of particles numerically. For

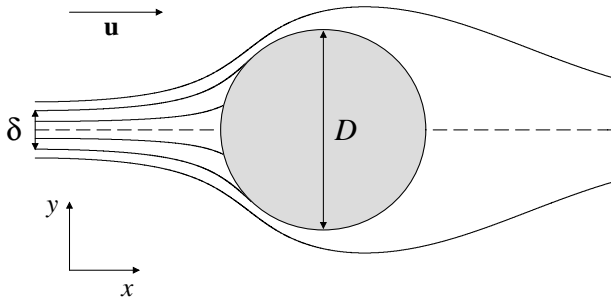


Fig. 2. The trajectories of particles released from different positions at the inlet of the periodic porous medium cell. $St = 0.25$ and the flow field \mathbf{u} is calculated from the analytical solution of Marshall *et al.* (24). The thick solid lines correspond to the limiting trajectories that determine δ .

simplicity, we assume that the influx of suspended particles is so small that (i) the fluid phase is not affected by changes in the particle volume fraction, and (ii) particle-particle interactions are negligible. Moreover, we also consider that the movement of the particles does not impart momentum to the flow field. Finally, if we assume that the drag force and gravity are the only relevant forces acting on the particles, their trajectories can be calculated by integration of the following equation of motion $\frac{d\mathbf{u}_p^*}{dt^*} = \frac{(\mathbf{u}^* - \mathbf{u}_p^*)}{St} + F_g \frac{\mathbf{g}}{|\mathbf{g}|}$, where $F_g \equiv (\rho_p - \rho)\ell|\mathbf{g}|/(V^2\rho_p)$ is a dimensionless parameter, \mathbf{g} is gravity, t^* is a dimensionless time, and \mathbf{u}_p^* and \mathbf{u}^* are the dimensionless velocities of the particle and the fluid, respectively.

We show in Fig. 2 some trajectories calculated for particles released in the flow for $St = 0.25$. Once a particle touches the boundary of the obstacle, it gets trapped. Our objective here is to search for the position y_0 of release at the inlet of the unit cell ($x_0 = 0$) and above the horizontal axis (the dashed line in Fig. 2), below which the particle is always captured and above which the particle can always escape from the system. As depicted in Fig. 2, the particle capture efficiency can be straightforwardly defined as $\delta \equiv 2y_0$. In the limiting case where $St \rightarrow \infty$, since the particles move ballistically towards the obstacle, the particle efficiency reaches its maximum, $\delta = D$. For $St \rightarrow 0$, on the other hand, the efficiency is smallest, $\delta = 0$. In this last situation, the particles can be considered as tracers that follow exactly the streamlines of the flow and are therefore not trapped.

We show in Fig. 3 the log-log plot of the variation of δ/D with the rescaled Stokes number in the presence of gravity for three different porosities. In all cases, the variable δ increases linearly with St to

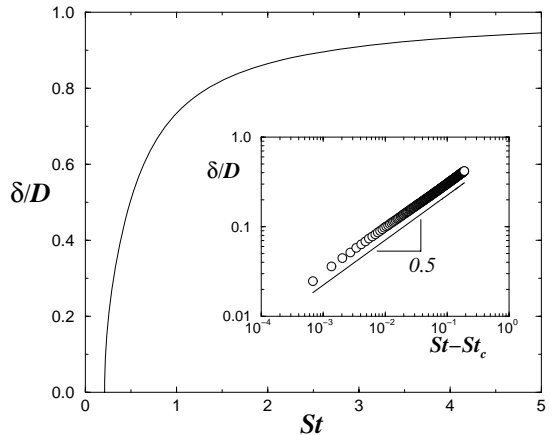


Fig. 3. The dependence of the capture efficiency δ on the rescaled Stokes number $St/(\epsilon - \epsilon_{min})$ for periodic porous media in the presence of gravity. Here we use $F_g = 16$, a value that is compatible with the experimental setup described in Ref. (19). The inset shows that the behavior of the system without gravity can be characterized as a second order transition, $\delta \sim (St - St_c)^\alpha$, with $\alpha \approx 0.5$ and $St_c = 0.2679 \pm 0.0001$, 0.2096 ± 0.0001 and 0.1641 ± 0.0001 , for $\epsilon = 0.85$, 0.9 and 0.95 , respectively.

subsequently reach a crossover at St_x , and finally approach its upper limit ($\delta = D$). The results of our simulations also show that $St_x \sim (\epsilon - \epsilon_{min})$, where ϵ_{min} corresponds to the minimum porosity below which the distance between inlet and obstacle is too small for a massive particle to deviate from the obstacle. The collapse of all data shown in Fig. 3 confirms the validity of the scaling law.

We see in the inset of Fig. 3 that the behavior of the system in terms of particle capture becomes significantly different in the absence of gravity. The efficiency δ remains equal to zero up to a certain critical Stokes number, St_c , that corresponds to the maximum value of St below which particles cannot be captured, regardless of the position y_0 at which they have been released. Right above St_c , the variation of δ can be described in terms of a power-law, $\delta \sim (St - St_c)^\alpha$, with an exponent $\alpha \approx 0.5$. Our results show that, while the exponent α is practically independent of the porosity for $\epsilon > 0.8$, the critical Stokes number decreases with ϵ , and therefore with the distance from the obstacle where the particle is released (see Fig. 3). To our knowledge, this behavior, that is typical of a second order transition, has never been reported before for inertial capture of particles. In order to have a more realistic model for the porous structure we did also include disor-

der (23). Here we adopted a random pore space geometry (17) shown in Fig. 1 and obtained the same results as for the regular case.

3. Conclusion and Outlook

We have found (16) that although the distribution of channel widths in a porous medium made by a two-dimensional RSA process is rather complex and exhibits a crossover at $l \sim D$, the distribution of fluxes through these channels shows an astonishingly simple behavior, namely a square-root stretched exponential distribution that scales in a simple way with the porosity. Future tasks consist in generalizing these studies to higher Reynolds numbers, other types of disorder and three dimensional models of porous media.

We also presented results for the inertial capture of particles in two-dimensional periodic as well as random porous media (23). For the periodic model in the absence of gravity, there exists a finite Stokes number below which particles never get trapped. Furthermore, our results indicate that the transition from non-trapping to trapping with the Stokes number is of second order with a scaling exponent $\alpha \approx 0.5$. In the presence of gravity, we show that (i) this non-trapping regime is suppressed (i.e., $St_c = 0$) and (ii) the scaling exponent changes to $\alpha \approx 1$. We intend to investigate in the future the possibility of non-trapping at first contact and the effect on the capture efficiency of simultaneous multiple particle release.

Acknowledgements

We thank the Max Planck Prize for financial support.

References

- [1] S.L. Soo, *Particles and Continuum: Multiphase Fluid Dynamics* (Hemisphere, New York, 1989).
- [2] D. Gidaspow, *Multiphase Flow and Fluidization* (Academic Press, San Diego, 1994).
- [3] K. Pye and H. Tsoar, *Aeolian sand and sand dunes* (Unwin Hyman, London, 1990).
- [4] F. A. L. Dullien, *Porous Media - Fluid Transport and Pore Structure* (Academic, New York, 1979).
- [5] P. M. Adler, *Porous Media: Geometry and Transport* (Butterworth-Heinemann, Stoneham MA, 1992).
- [6] M. Sahimi, *Flow and Transport in Porous Media and Fractured Rock* (VCH, Boston, 1995).
- [7] FLUENT (trademark of FLUENT Inc.) is a commercial package for computational fluid dynamics.
- [8] S. N. Coppersmith, C.-h. Liu, S. Majumdar, O. Narayan and T. A. Witten, *Phys. Rev. E* **53** (1996) 4673.
- [9] A. Cancelliere, C. Chang, E. Foti, D. H. Rothman, and S. Succi, *Phys. Fluids A* **2** (1990) 2085.
- [10] S. Kostek, L. M. Schwartz, and D. L. Johnson, *Phys. Rev. B* **45** 186 (1992).
- [11] N. S. Martys, S. Torquato, and D. P. Bentz, *Phys. Rev. E* **50** (1994) 403.
- [12] J. S. Andrade Jr., D. A. Street, T. Shinohara, Y. Shibusa, and Y. Arai, *Phys. Rev. E.* **51** (1995) 5725.
- [13] A. Koponen, M. Kataja, and J. Timonen, *Phys. Rev. E* **56** (1997) 3319.
- [14] S. Rojas and J. Koplik, *Phys. Rev E* **58** (1998) 4776.
- [15] J. S. Andrade Jr., U. M. S. Costa, M. P. Almeida, H. A. Makse, and H. E. Stanley, *Phys. Rev. Lett.* **82** (1999) 5249.
- [16] A.D. Araújo, W.B. Bastos, J.S. Andrade Jr. and H.J. Herrmann, accepted for *Phys. Rev. E*, physics/0511085
- [17] S. Torquato, *Random Heterogeneous Materials: Microstructure and Macroscopic Properties* (Springer, New York, 2002).
- [18] C. Tien, *Granular Filtration of Aerosols and Hydrosols* (Butterworths, Boston, 1989).
- [19] C. Ghidaglia, L. de Arcangelis, J. Hinch and E. Guazzelli, *Phys. Rev. E* **53** (1996) R3028 ; *Phys. Fluids* **8** (1996) 6.
- [20] J. Lee and J. Koplik, *Phys. Fluids* **13** 1076 (2001).
- [21] D. L. Koch and R. J. Hill, *Annu. Rev. Fluid Mech.* **33** (2001) 619.
- [22] D. E. Rosner and P. Tandon, *Chemical Engineering Science* **50** (1995) 3409.
- [23] A.D. Araújo, J.S. Andrade Jr. and H.J. Herrmann, preprint
- [24] H. Marshall, M. Sahraoui and M. Kaviany, *Phys. Fluids* **6** (1993) 507.